Are constant loop widths an artifact of the background and the spatial resolution?

M. C. López Fuentes[1,2,3], P. Démoulin[4], J. A. Klimchuk[2]

ABSTRACT

We study the effect of the coronal background in the determination of the diameter of EUV loops, and we analyze the suitability of the procedure followed in a previous paper (López Fuentes, Klimchuk & Démoulin 2006) for characterizing their expansion properties. For the analysis we create different synthetic loops and we place them on real backgrounds from data obtained with the Transition Region and Coronal Explorer (*TRACE*). We apply to these loops the same procedure followed in our previous works, and we compare the results with real loop observations. We demonstrate that the procedure allows us to distinguish constant width loops from loops that expand appreciably with height, as predicted by simple force-free field models. This holds even for loops near the resolution limit. The procedure can easily determine when loops are below resolution limit and therefore not reliably measured. We find that small-scale variations in the measured loop width are likely due to imperfections in the background subtraction. The greatest errors occur in especially narrow loops and in places where the background is especially bright relative to the loop. We stress, however, that these effects do not impact the ability to measure large-scale variations. The result that observed loops do not expand systematically with height is robust.

Subject headings: Sun: corona – Sun: magnetic fields – Sun: UV radiation

[1]Instituto de Astronomía y Física del Espacio, CONICET-UBA, CC. 67, Suc. 28, 1428 Buenos Aires, Argentina

[2]Naval Research Laboratory, Code 7675, Washington, DC 20375

[3]Member of the Carrera del Investigador Científico, Consejo Nacional de Investigaciones Científicas y Técnicas, Argentina

[4]Observatoire de Paris, LESIA, UMR 8109 (CNRS), F-92195, Meudon Principal Cedex, France

1. Introduction

Since the solar corona is optically thin, studies based on coronal loop observations must include some form of subtraction of the background contribution (see e.g., Klimchuk 2000, Schmelz & Martens 2006, López Fuentes, Klimchuk & Démoulin 2006). In their recent statistical study based on observations from the Transition Region and Coronal Explorer (*TRACE*, see Handy et al. 1999), Aschwanden, Nightingale & Boerner (2007) showed that the background can be several times brighter than the loops themselves. It is likely that the background corona is formed by a number of loops that are too faint to produce a large enough contrast to make them detectable. However, these unobserved structures constitute a spatially fluctuating background for actual observed loops. Therefore, even for loops with constant intensity along their length, fluctuations due to the structuring of the background are expected. The determination of morphological properties of a loop, such as its diameter, can be affected by the characteristics of the background, and therefore it is important that the background be taken into account during such analyses.

In a recent paper (López Fuentes, Klimchuk & Démoulin 2006, henceforth LKD06) we explored the problem of the apparent constant width of coronal loops. Since loops are the trace of magnetic flux tubes rooted in the photosphere, we might expect on the basis of simple force-free magnetic field models that most loops would expand with height. However, observations show that this is not the case; both X-ray loops (Klimchuk 2000) observed with the Soft X-ray Telescope (SXT, see Tsuneta et al. 1991) aboard Yohkoh, and EUV loops (Watko & Klimchuk 2000, and LKD06) observed with *TRACE*, seem to correspond to constant cross-sections.

In LKD06, we compared a number of observed *TRACE* loops with corresponding model flux tubes obtained from force-free extrapolations of magnetogram data from the Michelson Doppler Imager (MDI, see Scherrer et al. 1995) aboard the Solar and Heliospheric Observatory (*SOHO*). To quantify the expansion of the loops and flux tubes, we defined the expansion factor Γ as the ratio between the widths averaged over the middle and footpoint sections. We found that the mean expansion factor of the model flux tubes is about twice that of the corresponding observed loops. Another important result is that the cross section is much more asymmetric (from footpoint to footpoint) for the model flux tubes than for observed loops. We suggest that the origin of this asymmetry lies is the complexity of the magnetic connectivity of the solar atmosphere. In LKD06 we proposed a mechanism to explain the observed symmetry of real loops.

Although the measured widths of observed loops have very little global variation, there are short distance fluctuations as large as 25% of the average width. In LKD06 the loop background was subtracted by linearly interpolating between the intensities on either side

of the loop. Since the background intensity can be as much as three to five times the intrinsic intensity of the loop, we might expect the width determination to be less reliable at positions where the ratio of loop to background intensities is smaller. If so, then measured width variations might be partly or largely an artifact of imperfect background subtraction.

It is also possible that the width fluctuations are indicative of real structural properties of the loops. For instance, loops may be bundles of thinner unresolved magnetic strands that wrap around each other. If there are only a few such strands, then we might expect the width of the bundle to fluctuate on top of a global trend. Furthermore, the width should be anti-correlated with the intensity, since the bundle will be thinner and brighter in places where the strands are lined up along the line of sight, and it will be fatter and fainter in places where the stands are side-by-side across the plane of the sky.

The filamentary nature of coronal loops, and the solar corona in general, has been progressively evident from the combination of models and observations (for a review, see e.g., Klimchuk 2006). Our ability to discern the internal structure of loops is limited by the instrument resolution. It can be seen from *TRACE* images that structures many times wider than the instrument Point Spread Function (PSF) are clearly made of thinner strands. It is not surprising then that recognizable "individual" loops are no thicker than a few times the PSF width. Since identifiable individual loops are close to the resolution limit, it has been suggested that the apparent constant width may just be an artifact of the resolution (see the recent paper by DeForest 2007). If loops are everywhere much smaller than the PSF, then they will appear to have a constant width equal to that of the PSF, even if the true width is varying greatly. We have carefully accounted for the PSF in our earlier studies and concluded that this is not a viable explanation for the observed constant widths. What we have not addressed in as much detail is the possible role of imperfect background subtraction. This paper describes a study that addresses both the background subtraction and finite resolution and the extent to which they influence the measured widths of loops.

Our approach is to produce synthetic loops with constant and variable cross-sections, and place them on real *TRACE* backgrounds to simulate loop observations. We then process the synthetic data following the same procedure used in LKD06, so we can compare them with actual *TRACE* loops. This allows us to determine whether the procedure followed in LKD06 is able to distinguish expanding loops from constant cross-section loops. We will answer the question of whether the lack of global expansion in observed loops is real or simply an observational artifact, as suggest by DeForest (2007). We will also investigate the reliability of the shorter length scale fluctuations that are often observed.

In Section 2 we describe the main properties of the set of loops studied in LKD06. We explain the synthetic loop construction in Section 3. In Section 4 we compare synthetic and

observed loops, and we discuss and conclude in Section 5.

2. Observed *TRACE* loops

In LKD06 we studied a set of 20 loops from *TRACE* images in the 171 Å passband. To determine the width of the loops we followed a procedure based on the measurement of the second moment (the standard deviation) of the cross-axis intensity profile at each position along the loop. The measurement is done on a straightened version of the loop, as described in LKD06. Assuming circular cross-sections and uniform emissivity, the cross-section diameter (that we refer to as the width) will be 4 times the standard deviation of the profile. The same procedure had been used in previous studies (see Klimchuk et al. 1992, Klimchuk 2000, Watko & Klimchuk 2000). The actual background is estimated by linear interpolation of the background pixels at both sides of the loop. The obtained width is corrected for instrumental resolution (i.e. the combined PSF due to telescope smearing and detector pixelation).

The typical length of the studied loops is around 150 *TRACE* pixels or 54 Mm, though loops as long as 300 pixels (108 Mm) are included in the set. The average width for all loops in the set is 4.2 pixels or 1.5 Mm. Figure 1 shows a typical case having the average width and length. The upper panel shows the loop as observed in the *TRACE* image, and the lower panel is the "straightened" version.

For the resolution correction we use a conversion curve (see Figure 4 in LKD06) to transform each measured standard deviation value to width. The curve has been obtained assuming a Gaussian PSF with a full width at half maximum of 2.25 pixels and loop cross-sections that are circular and uniformly filled. The chosen PSF width is an upper limit for values obtained in different studies (Golub et al. 1999, Gburek, Sylwester & Martens 2006). The resolution correction curve plays a two-fold role. First, it allows us to obtain a more realistic width value from a measured quantity like the standard deviation. Second, it is a filter for measurements that are clearly unreliable. Standard deviation measurements smaller than a minimum value equal to the standard deviation of the PSF itself (where the conversion curve crosses the abscissa axis, see LKD06 Figure 4) are considered untrustworthy, and the corresponding width is set to zero (i.e., rejected). Problems resulting from significant errors in the background subtraction can also be identified in this way. It is worth remarking that our approach is quite cautious in that the PSF we have assumed is wider than the most recent estimates (see Gburek, Sylwester & Martens 2006). Some of the measurements we reject as being unresolved may in fact be valid.

Figure 2 is a plot of width (asterisks) versus position along the loop shown in Figure 1. The horizontal line corresponds to the average width. It is nearly identical to the mean width of all the loops in the set. The three "zero width" values that lie on the abscissa axis correspond to standard deviation measurements that were below the resolution limit as explained above.

To quantify the expansion of loops from footpoint to top we defined expansion factors as follows:

$$\Gamma_{m/se} = \frac{2\ W_m}{W_s + W_e}, \quad \Gamma_{m/s} = \frac{W_m}{W_s} \quad \text{and} \quad \Gamma_{m/e} = \frac{W_m}{W_e}, \tag{1}$$

where W_m, W_s and W_e are the average width of portions that cover 15% of the loop length at the middle, start footpoint, and end footpoint, respectively. Start and end refer to the magnetic field line traces used to define the magnetic flux tubes in the extrapolation models. The model flux tubes expand much more than the corresponding observed loops (LKD06). Their expansion factors are 1.5 to 2 times larger.

As explained in Section 1, the loop width fluctuates as much as 25% over short distances (see e.g., Figure 2). We tried alternate measures of the loop width (full width at half maximum and equivalent width of the intensity profile), and the same fluctuations are present. Our conclusion is that the fluctuations are most likely due to the influence of the background (see below). Since these fluctuations have a short length scale and vary quasi randomly around a global trend, they do not significantly affect the measured expansion factors.

3. Synthetic loops

In this study we create a set of synthetic loops with similar characteristics to the *TRACE* loops studied in LKD06, and we overlay them on real *TRACE* backgrounds. The axis of the loop is linear and its cross-section is circular. To analyze the possibility that the apparent constant width is due to a resolution effect we create loops of two kinds: loops with constant diameter along their length, and loops that are wider in the middle than at the footpoints. For the second class of synthetic loops we use an expansion factor that is typical of the model flux tubes obtained in LKD06. We set the diameter of the loop at the mid point to be twice the diameter at the ends, and we assume that the diameter varies quadratically with position. Since the expansion factor defined in Equation (1) involves averages along 15% sections of the loop, $\Gamma_{m/se} = 1.57$ rather than 2.0.

We have chosen two kinds of background for the synthetic loops. Background I, shown in the top-left panel in Figure 3, corresponds to a typical *TRACE* loop background: it has similar intensity magnitude and fluctuations, and it contains moss (see Berger et al. 1999, Martens et al. 2000) and other intense features. Background II, shown in the top-right panel, is fainter and fluctuates less than Background I. Although it does not correspond very well to real loop backgrounds, we consider it interesting to study how this kind of background affects the width determination. The average intensities of backgrounds I and II are approximately 70 and 30 DN (Data Numbers), respectively. For comparison, the typical intrinsic (background subtracted) intensity of observed loops is between 20 and 40 DN. Both background areas have been extracted from a *TRACE* image in the 171 Å band obtained at 01:45 UT on July 30, 2002.

To create a simulated *TRACE* image containing the synthetic loop we proceed as follows. We create an image of the loop without background. The maximum intensity of the loop (at the axis) is set proportional to the average intensity of the background image on which it will be later superposed. The constant of proportionality is referred to as the intensity factor Φ. Since the background intensity tends to be higher than the intrinsic loop intensity, Φ is generally smaller than 1. To simulate the finite resolution, we smooth the image of the loop using a gaussian profile with a full width at half maximum of 2.25 pixels corresponding to the instrument PSF. The resulting loop is then placed on the previously selected background (I or II) from the *TRACE* image.

The images in Figure 3 have been created as described above. Both panels in each row use the same synthetic loop placed in one case on background I (left) and the other case on Background II (right). The four loops differ in the following ways. The loop in the second row (panels a and b) has a constant diameter of 4 pixels, corresponding to $\Gamma_{m/se} = 1$. The loop in the third row (panels c and d) has a diameter that expands from 2.5 pixels at the ends to 5 pixels at the center, corresponding to $\Gamma_{m/se} = 1.57$. The loop in fourth row (panels e and f) has a constant diameter of 3 pixels. Finally, the loop in the bottom row (panels g and h) expands from 2 pixels at the ends to 4 pixels in the middle. Notice that the ends of this last loop are narrower than the PSF. The intensity factor Φ has been adjusted so that the resulting loops look similar, by eye, to typical *TRACE* loops. We used $\Phi = 0.5$ for Background I and $\Phi = 0.7$ for Background II. Considering the average intensities of Backgrounds I and II, this gives intrinsic loop intensities of around 35 DN and 25 DN, respectively. These values are consistent with the intrinsic intensities of observed loops.

The photon statistical noise associated with *TRACE* data is given by $\sqrt{N}$, where N is the number of photon counts per pixel (Handy et al. 1999). Since 1 DN corresponds to 12 photon counts, the photon noise as a percentage of the signal is:

$$PN_{\%} = 100\frac{\sqrt{12I}}{12I} \approx \frac{30}{\sqrt{I}}, \tag{2}$$

where I is the intensity of the signal in DN/pix. The synthetic loop data constructed here includes the photon noise present in the *TRACE* image used for the background. As we now demonstrate, this contribution dominates the noise from the loop itself, so we can safely ignore the loop contribution. Let us first consider the extreme case of low background and loop intensities, namely: $I_b = 30$ DN and $I_l = 10$ DN. According to Equation (2) the photon noise of the total signal is $PN_{\%} = 30/\sqrt{40}$ or 4.7%. On the other hand, for our synthetic images (photon noise from the background only) it is $PN_{\%} = 30/\sqrt{30}$ or 4.1%, meaning a difference of 0.6%. For a more typical case of $I_b = 70$ DN and $I_l = 25$ DN, the same percentages are 3.1% and 2.6% respectively, implying a difference of 0.5% of the total signal. These differences are minor and will have a negligible effect on the results of the following sections.

4. Results

4.1. Can we detect expanding loops?

From the set of loop images, we measured the width following the same procedure used in LKD06 for real loops and described in Section 2. We used the conversion curve (Figure 4 in LKD06) to correct for the instrument PSF. The non-linearity of the curve increases the dispersion of the resulting widths at smaller values approaching the width of the PSF. In Figure 4 we plot the "measured" width (asterisks) versus position along the loop for the eight cases in Figure 3. The format of the figures is the same. For comparison, we also plot as continuous lines the actual diameters used to construct the images. It can be seen that, despite the fluctuations, expanding and constant width loops are clearly distinguishable. This is true for loops that are relatively wide (top two rows) and loops that are relatively narrow (bottom two rows). This demonstrates convincingly that, if loops expanded as expected from standard force-free extrapolation models, then it would be noticeable from observations even when they are very close to the resolution limit (last row). Since that it not the case, this may imply that actual magnetic fields have more complexity than is present in the standard models. We know, for example, that the field is comprised of many thin flux strands (elemental kilogauss tubes) that are tangled by photospheric convection. We believe this can explain the symmetry of observed loops with respect to their summit (see discussion in LKD06 and Klimchuk 2006), but whether it can also explain the lack of a general expansion with height is unclear.

It is interesting to note from the plots in Figure 4 that the measured width is systematically smaller than the width set in the construction of the loops. This tendency appears in all loops and is very likely due to an underestimation of the real width in the measurement procedure. The procedure requires a subjective selection of the loop edges for the purpose of defining the background and computing the standard deviation. During this step one can miss the faint tail of the cross-axis intensity profile that blends in with the background. We have verified that there is a tendency to define the loop edges to be slightly inside the actual edges. This causes the measured width to be artificially small, both because the tail of the profile is missing from the standard deviation computation and because too strong a background is subtracted from the loop. We expect the effect to be greatest for loops that are especially faint or especially narrow, as discussed below. If this explanation is correct, we can conclude that the *TRACE* loops studied in LKD06 are actually slightly wider than our measurements seem to indicate.

The fact that the measured width is a lower bound for the real width gives further support to our assertion that the analyzed loops are instrumentally resolved. In LDK06, we estimated the width uncertainties associated with background subtraction by repeating each measurement using different choices for the loop edges. We concluded that rule-of-thumb error bars range from 10% below to 20% above the measured best value. It now appears that the actual error bars may be somewhat larger. However, we stress that this does not impact our ability to distinguish expanding loops from non-expanding loops, as is readily apparent from Figure 4.

To quantify this claim, we computed the expansion factors ($\Gamma_{m/se}$ in Equation 1) of all the synthetic loops shown in Figure 4. These are listed in Table 1. The upper and lower limits that define the error bars are the expansion factors $\Gamma_{m/s}$ and $\Gamma_{m/e}$. For comparison, in the case of the observed loop of Figures 1 and 2, the expansion factor computed in the same way is 1.03 ± 0.04. The values given in Table 1 clearly confirm our conclusion that loops with constant and expanding cross section can be easily distinguished. It is interesting to note that the expansion factors for the same loops placed in different backgrounds can be notably different. The same is true for loops of the same kind (expanding or not) but with different characteristic size (wide or narrow). Compare row 1 with row 3, and row 2 with row 4 in Figure 4 and the table. The error bars are also different in all cases. Part of these differences may be due to the subjective part of the analysis procedure (the selection of the loop edges). However, repeating the width measurements we obtain approximately the same expansion factors. Therefore, the distribution of the background emission and the characteristic size of the loop both play a role in determining the precise value of the expansion factors and the error bars. In particular, Backgrounds I and II tend to give an under and over estimation of the expansion factors, respectively (compared to the values set during the loop construction).

Nevertheless, we want to stress that the measured expansion factors of the expanding and non-expanding synthetic loops are clearly clustered around the actual values, implying that loops with constant and expanding cross section are readily distinguishable.

Next, we study how the observed loop expansion is affected by the relative intensity of the loop compared to the background. To test this, we created synthetic data in the way described in Section 3, for different values of the loop-to-background intensity ratio Φ. In Figure 5 we plot the expansion factor $\Gamma_{m/se}$ (Equation 1) versus Φ for 4 narrow synthetic loops with similar characteristics to those shown in panels e) to h) of Figures 3 and 4. The difference is that the loops of Figure 5 are 300 pixels long, instead of 200 pixels. The definition of Γ is not affected by the change of length. On the other hand, longer loops provide more measurements and better statistics for studying how loop expansion depends on the loop-to-background intensity ratio. We chose thin loops for Figure 5 because their expansion is more challenging to measure and they are more affected by the background.

If the intensity ratio Φ is too small, it is difficult to detect a loop above the background, much less measure its width. Our previous studies of observed loops have therefore avoided such cases. We subjectively define a lower limit for loop visibility of around $\Phi = 0.3$. Below that, the width determination is unreliable. The upper value $\Phi = 1.5$ is extreme for most *TRACE* loops, but it is interesting for analysis and may be appropriate to other datasets. The intermediate Φ values are 0.5, 0.7 and 1.0. Figure 5 provides strong additional support for our claim that the expansion factors of expanding and non-expanding loops can be clearly distinguished, even for the most critical cases of very low intensities and narrow widths. In no case do the error bars of expanding and non-expanding loops overlap.

It is interesting to note that the synthetic loops used for Figure 5 overlap with more of the background image than do the shorter synthetic loops used for Figures 3 and 4. The footpoint and middle sections therefore combine with different portions of the background. Since the expansion factors are qualitatively similar in the corresponding cases, we can be confident that our results are not an artifact of the particular loop-background combinations.

So far we have not considered loops that are completely below the resolution limit. In Figure 6 we show two cases of unresolved synthetic loops. Both have a constant diameter of 0.5 pix, and both use Background I (Figure 3). The loops differ only in the intensity ratio Φ, which is set to 1 for case (a) and 3 for case (b). Note, however, that because the loops occupy only a fraction of a pixel, the "observed" intensity ratios are much smaller: around 0.25 for the Φ=1 loop and 0.5 for the Φ=3 loop.

Figure 7 shows the widths of the loops as measured in the usual way, including correction for instrument resolution. A majority of the measurements are equal to zero, meaning that

the computed standard deviation is below that of the PSF. This is especially true for the fainter loop of case (a). We can understand this behavior as follows. Due to the influence of the variable background, we expect some measurements to be too large and others to be too small. However, because of the systematic effects associated with loop edge selection, discussed above, we expect more of the measurements to be too small.

The conversion from standard deviation to width is very sensitive at small values, where the conversion curve is nonlinear, and it only takes small errors in the standard deviation to produce a zero width value. The solid line in Figure 7 indicates the actual loop width of 0.5 pix, while the dashed line indicates the full width at half maximum of the PSF. The most important conclusion to draw from the figure is that our measurement technique can easily detect when loops are unresolved, i.e., when they are thinner than the PSF. As we stated before, the loops analyzed in LKD06 and previous works are all wider than the PSF (see also Section 5 below).

Finally, in Figure 8 we plot width versus position along a synthetic loop with a footpoint width of 2.5 pixels and a model expansion factor of $\Gamma_{m/se} = 2.2$. Our measurement procedure tracks the loop expansion very well. The expansion factor computed from the observed width as in Table 1 gives $\Gamma_{m/se} = 2.1 \pm 0.2$. Therefore, the loop can be readily distinguished from the $\Gamma_{m/se} = 1.57$ loop having the same footpoint size in Figure 4, panel (d).

4.2. Short length scale width fluctuations

As discussed in Section 1 the measured widths of observed loops fluctuate as much as 25% over short length scales. It is important to know whether these variations are real or an artifact of the background. Comparison of panels a) and b) in Figure 4 with Figure 2 shows that synthetic and observed loops with similar characteristic width exhibit similar width fluctuations. For the observed loop of Figure 2, the amplitude of the fluctuations computed as the ratio of the standard deviation of the measured width to its average is 18%. The corresponding ratios for the synthetic loops of panels (a) and (b) in Figure 4, are 17% and 25%, respectively. This suggests that the fluctuations are not real and argues against loops being comprised of a small number of braided strands (the possibility that they are bundles of *many* tangled strands is not affected). This is not a firm conclusion, however, since the fluctuations are somewhat more coherent for the observed loop than for the synthetic loop. We return to this issue below. Narrower loops (e.g., panels (e) and (f) in Figure 4) show larger amplitude fluctuations (21% and 38%, respectively) mostly because of the non-linearity of the resolution correction curve (LKD06 Figure 4), which exaggerates differences at smaller widths.

To study how the background fluctuations affect the width determination, we analyze the relationships between the width and the loop and background intensities. In Figure 9 we plot as a function of position along the loop: the intensity of the background pixels at either side of the loop (from which the loop background is linearly interpolated; continuous lines), the loop width (dotted), the loop intensity (maximum intensity of the background-subtracted profile; dashed), and the absolute value of the difference between the two background pixel intensities (dot-dashed). The loop width is given in pixels and multiplied by 10 for easier comparison with the intensities. The upper panel corresponds to the observed loop example of Figures 1 and 2, and the lower panel correspond to the synthetic loop of Figures 3 and 4, panels (a).

Figure 9 shows that our synthetic loop data share the main qualitative characteristics of real loops. The fluctuations of the background intensity and its difference at the sides of the loop, and the loop intrinsic intensity and its fluctuations, are similar in both cases. There are obvious differences due to the spatial structure unique to each background that can easily be identified in the images. For example, the bumps between 30 and 60 for the observed loop, and between positions 0 and 40 and between 90 and 130 for the synthetic loop, can be traced to patches of enhanced emission in Figures 1 and 3. Another difference is the global variation in the intensity of the observed and synthetic loops. The measured intensity of the synthetic loop is nearly constant because the loop was constructed that way (small fluctuations come entirely from imperfect background subtraction). The measured intensity of the observed loop, on the other hand, tends to diminish systematically toward the right end. This is likely to be real and not an artifact of the background subtraction. Despite of these expected differences, the comparison shows that the synthetic loops reproduce the main properties of the observed cases.

We have suggested that small-scale fluctuations of the measured intensities and widths of loops are due to imperfect background subtraction. To further assess this, we look for statistical correlations between these quantities. In the upper panels of Figure 10 we plot width versus intensity for all positions along the observed and synthetic loops, respectively. We find that there is a small direct correlation between the width and intensity in both cases: wider sections of the loops tend to be brighter. The lines in the scatter plots are least-squares fits, which have the indicated slopes and intercepts. The correlation between width and intensity can be explained by the tendency, during the interactive analysis procedure, to miss the wings of the intensity profile and define the loop edges to be inside the true edges. As described earlier, this causes an over estimation of the background intensity and produces artificially narrow loop widths and artificially faint loop intensities. We expect the magnitude of this effect to vary depending on the brightness of the background relative to the loop. It will be stronger (i.e., the underestimates of width and intensity will be greater)

when the background is relatively bright. This is confirmed in the second row of Figure 10. It shows an inverse correlation between the measured width and the background-to-loop intensity ratio for both the observed and synthetic loops. The background intensity used here is the average of the sloping background subtracted during the analysis (i.e., the average of the values on either side of the loop). Notice also that for the synthetic loop, the measured width tends to be smaller than the model width (4 pixels) when the relative intensity of the background is larger.

This effect is almost certainly responsible for the width-intensity correlation of the synthetic loop and seems a likely explanation for the observed loop, as well. Whether it is strong enough to allow the possibility that loops are bundles of a few (3-5) intertwined strands is unclear. Recall that such loops would exhibit an inverse correlation between width and intensity if the measurements were perfect. Are measurement errors large enough to negate this inverse correlation and produce a small direct correlation, as observed? Only more involved modeling can answer this question.

It seems plausible that cross-loop gradients in the background could also have an effect on the measured width. Certainly small scale inhomogeneities are more difficult to subtract than a flat background. In the upper panels of Figure 11, we plot width versus the absolute value of the background intensity difference on the two sides of the loop. No correlation is apparent for either the observed or synthetic loops. We confirmed a lack of correlation using a non-parametric statistical analysis. We also find no correlation between the intrinsic loop intensity and the background intensity difference.

The right bottom panel of Figure 11 indicates how the known error in width measurement for the synthetic loop correlates with the background intensity gradient. The ordinate is the absolute value of the difference between the measured width and the width used during the loop construction. The abscissa is the absolute value of the background intensity difference on the two sides, normalized by the loop intensity. The normalization is meant to compensate for the fact that background gradients should have a lesser impact on bright loops. The left bottom panel of Figure 11 is a corresponding scatter plot for the observed loop. Since the actual width is not known, the ordinate is replaced by the absolute value of the deviation of the measured width from its mean. In neither case is there a correlation, as confirmed by statistical analysis. We conclude that the magnitude of the background has a bigger effect on the width measurements than does the difference in the background on the two sides of the loop (the cross loop gradient).

5. Discussion and conclusion

In this paper we study the effect of the background and the instrument PSF in the determination of the apparent width of EUV coronal loops observed by *TRACE*. Our main motivation is to extend the results obtained in our previous work: López Fuentes, Klimchuk & Démoulin (2006; LKD06). There, we compared a set of observed *TRACE* loops with corresponding force-free model flux-tubes, and we found that observed loops do not expand with height as expected from the extrapolation model. Here, we construct artificial loops with expansion factors similar to those of the studied loops and the model flux-tubes, and we overlay them on real *TRACE* backgrounds. We repeat on these synthetic loops the same procedure followed in LKD06, and compare the results back with real loops. We find that even for loops close to the resolution limit the procedure followed in LKD06 discerns expanding and non-expanding cross-sections. The method includes a resolution correction that identifies measurements that are below the resolution limit and therefore unreliable (see explanation in Section 2). We used a gaussian Point Spread Function (PSF) for the instrument with a FWHM of 2.25 pixels, which is an upper bound for values found by different authors (Golub et al. 1999, Gburek et al. 2006).

In a recent paper, DeForest (2007) has proposed the interesting idea that most thin individual loops observed by *TRACE* are actually extremely bright structures well under the resolution limit. In this scenario, the loop apparent width would be given by the instrument PSF. In this way, loops may actually expand, but their size both at the top and the footpoints would be unresolved and would appear the same. The motivations for this conjecture are the apparent constant width of loops, and the observation that *TRACE* loops have an intensity scale height that is considerably larger than expected for static equilibrium (Winebarger et al. 2003, Aschwanden et al. 2001) or steady flow (Patsourakos & Klimchuk 2004). More precisely, for expanding loops that are everywhere unresolved, the density gradient present in the corona is larger than inferred from the observations under the assumption of constant cross section.

According to the above explanation, we should expect all individual *TRACE* loops to have a true width less than that of the PSF and an apparent width roughly equal to that of the PSF. However, observations do not support this. The mean width of the loops studied in LKD06 is 4.2 pix after correction for the instrument resolution (see also Watko & Klimchuk 2000). As shown in Figure 7 and discussed in Section 4.1, our method can easily identify loops that are intrinsically more narrow than the PSF. The loops selected for our studies are clearly not of this type.

As we discussed in Section 1, coronal structures that are many times wider than the *TRACE* PSF are observed to be formed by thinner individual loops. Therefore, there is an

intermediate range of widths – let us say between one and three PSF widths – for which the profiles produced by unresolved threads could overlap to form apparently wider loops. This, together with the effect of a fluctuating and intense background, are the arguments provided by DeForest (2007) to explain loops wider than the PSF. A key point in this discussion is that unresolved neighbor threads might be expected to separate from each other with height for the same reasons that individual strands might be expected to expand with height (e.g., if the field behaves like *simple* force-free extrapolation models predict). In this respect, a structure formed by diverging threads does not differ from the expanding loops studied in Section 3. As we discussed there, the plots in Figures 4 and 5 and the Γ factors given in Table 1 show clearly that our procedure for the width determination would be able to detect the expansion if it existed, even for loops near the resolution limit.

It is interesting to compare the synthetic images in Figure 2 in DeForest's article with our Figure 3. There, he claims that synthetic loops made from a single unresolved thread of constant width and from two diverging threads are indistinguishable from each other and from actual *TRACE* loops. In our Figure 3 it is also very difficult, by eyeball, to determine which loops have expanding widths or constant widths. However, the plots in Figure 4 show that a careful examination through a quantitative measurement provides the answer.

One of DeForest's main arguments is that it is difficult to measure the width of features that are at or near the instrument resolution due to effects such as the smearing from the telescope, pixilation from the detector, and the presence of background emission. We agree, but these claims need to be quantified. It is not sufficient to make eye-ball comparisons of features. Quantitative measures must be used. We have adopted the standard deviation of the loops cross-axis intensity profile as one such measure. We have been very careful in our work to indicate when the measurements are reliable and when they are not. Measured widths that are very close to the instrument resolution have very large error bars that we show (see LKD06) and that we take into account.

We have paid particularly careful attention to the effects of the combined PSF, which accounts for both smearing and pixilation. DeForest is correct that measurements of very thin features depend critically on the PSF. We have therefore adopted a conservative value for the PSF width that is greater than the estimates determined by the instrument teams and others. Furthermore, features as narrow as our assumed PSF are routinely observed, which would not be possible if the actual PSF were wider.

DeForest is also correct that background emission can be important and may lead to spurious results. It is therefore vital to subtract the background before making measurements, as we have done. In LKD06, we have avoided loops where the background is especially bright or complicated. We attempted in our earlier studies to estimate the uncertainties as-

sociated with imperfect background subtraction, but this was not as careful as our treatment of resolution effects. The main purpose of this paper was to rigorously evaluate the effects of background on the measurement of loop widths.

Regarding the importance of quantitative measurements versus visual inspection, we concur with DeForest that the visual determination of the edge of a feature is subjective and largely based on the intensity gradient across the feature. This can lead to erroneous conclusions about width variations if there is a systematic variation of intensity along the feature, such as decreasing intensity with height. Our quantitative measure of width based on the standard deviation of the intensity profile is by construction moderating such bias. The positive correlation found between the loop width and the maximum intensity (top panels in Figure 10) could be a remnant of this effect or an intrinsic property of the loops.

DeForest correctly points out that, with optically-thin coronal emission, the observed intensity scale height of a hydrostatic structure is larger for an expanding loop than for a constant cross section loop, especially if the loop is unresolved. In fact, for the 1-2 MK model examples he shows (Figures 5 and 6), the intensity actually increases with height by a factors of 2-3 to a maximum brightness at altitudes near 7×10^9 cm). Whether actual TRACE loops have this property is unknown and should be investigated. The variation of temperature with height combined with the transmission properties of the filter used will complicate the interpretation.

We note that the observation of super-hydrostatic scale heights is different from the observation of excess densities in TRACE loops. For most TRACE loops, the density inferred from the observed emission measure and diameter is much larger than that expected from static equilibrium theory, given the observed temperature and loop length (Aschwanden et al. 2001, Winebarger et al. 2003). DeForest's idea of unresolved loops would make this discrepancy even worse, since a higher density is required to produce the same emission measure from a smaller volume.

The loops identified and measured by DeForest are qualitatively much different from the loops identified and measured in our studies. We chose cases that are not obviously composed of a few resolved or quasi-resolved strands (although we believe that our loops may be composed of large numbers of elemental strands that are far below the resolution limit). The only one of his loops with no apparent internal structure (Loop 6 in his Figure 8) would have not been selected by us, because it is barely discernable above the background. On the other hand, some of the thinner structures within DeForest's loop bundles (e.g., at the bottom edge of his Loop 3) are not unlike the loops we have investigated. In this regard, we must clarify a comment attributed to one of us at the end of Section 5 in his paper. We suggest that researchers seeking to study monolithic-looking loops will tend to select cases

that are only a few resolution elements across. Significantly wider loops (e.g, all except Loop 6 in DeForest's sample) usually show evidence of internal structure and will be rejected.

We agree fully with DeForest that collections of loops (loop bundles) expand appreciably with height. However, we stand by our claim that individual loops that are clearly discernable within a bundle have a much more uniform width. This is not an artifact of the resolution. A hare and hounds exercise, as currently planned, is one useful way to clarify any remaining differences of opinion.

An important topic of the present study has been the analysis of how the properties of the background affect the loop width determination. We searched for correlations between the width and: the loop intrinsic intensity, the background intensity to loop intensity ratios, and the absolute value of the background difference. The background intensity is computed as the average between the pixels at both sides of the loop, which is used for the estimation of the actual loop background, while the background difference is the difference between those pixels. We found a direct correlation between the width and the maximum intensity of the loop profile (see Figure 10, upper panels). This is probably due to the fact that we tend to miss the "tails" of the loop profile at positions where the loop is less intense with respect to the background, and therefore, the measured profile tends to be narrower. This is confirmed by the inverse correlation found between the width and the ratio of background intensity to loop intensity (see Figure 10, bottom panels). It can be seen from the plots that the width tends to be abnormally narrower, and the points more disperse, for larger background to loop intensity ratios.

We found no evidence of correlation between the width and the the background difference. This shows that the background gradients are less important in the determination of the width than the background relative intensity. We stress, however, that this does not affect our ability to determine the global expansion properties of loops, and that despite of the background contribution we are readily able to distinguish constant width loops from loops that expand as predicted from simple force-free magnetic models.

The results presented here are extremely intriguing and provide clues and new questions to guide future investigations. However, it is expected that definitive answers will come from improved observations using new generations of solar instruments with higher resolution.

We acknowledge the Transition Region and Coronal Explorer (*TRACE*) team. We wish to thank Craig DeForest for fruitful discussions about the nature of observed loops. We also thank our anonymous referee for his/her valuable suggestions and comments. The authors acknowledge financial support from CNRS (France) and CONICET (Argentina) through their cooperative science program (N^0 20326). MLF thanks the Secretary of Science and

Technology of Argentina, through its RAICES program, for travel support. This work was partially funded by NASA and the Office of Naval Research.

REFERENCES

Aschwanden,M.J., Nightingale,R.W., & Boerner,P. 2007, ApJ, 656, 577

Aschwanden, M. J., Schrijver, C. J., & Alexander, D. 2001, ApJ, 550, 1036

Berger, T. E., De Pontieu, B., Fletcher, L., Schrijver, C. J., Tarbell, T. D., & Title, A. M. 1999, Sol. Phys., 190, 409

DeForest, C. E. 2007, ApJ, 661, 532

Gburek, S., Sylwester, J., & Martens, P. 2006, Sol. Phys., 239, 531

Golub, L., et al. 1999, Physics of Plasmas, 6, 2205

Handy, B. N., et al. 1999, Sol. Phys., 187, 229

Klimchuk, J. A. 2000, Sol. Phys., 193, 53

Klimchuk, J. A., Antiochos, S. K., & Norton, D. 2000, ApJ, 542, 504

Klimchuk, J. A. 2006, Sol. Phys., 234, 41

Klimchuk, J. A., Lemen, J. R., Feldman, U., Tsuneta, S., & Uchida, Y. 1992, PASJ, 44, L181

López Fuentes, M. C., Klimchuk, J. A., & Démoulin, P. 2006, ApJ, 639, 459 (LKD06)

Martens, P. C. H., Kankelborg, C. C., & Berger, T. E. 2000, ApJ, 537, 471

Patsourakos, S. & Klimchuk, J. A. 2004, ApJ, 603, 322

Scherrer, P. H. et al. 1995, Sol. Phys., 162, 129

Schmelz, J. T., & Martens, P. C. H. 2006, ApJ, 636, L49

Watko, J. A. & Klimchuk, J. A. 2000, Sol. Phys., 193, 77

Winebarger, A. R., Warren, H. P., & Mariska, J. T. 2003, ApJ, 587, 439

Table 1: Expansion factors $\Gamma_{m/se}$ (Equation 1) for the synthetic loops shown in Figures 3 and 4 (see detailed explanation in Section 4.1).

Synthetic loop	Imposed	Background I	Background II
Const. width (4 pix)	1	$0.85 \pm .02$	$0.95 \pm .04$
Variable width (2.5-5 pix)	1.57	$1.38 \pm .25$	$1.76 \pm .01$
Const. width (3 pix)	1	$0.82 \pm .05$	$1.03 \pm .03$
Variable width (2-4 pix)	1.57	$1.59 \pm .28$	$2.11 \pm .20$

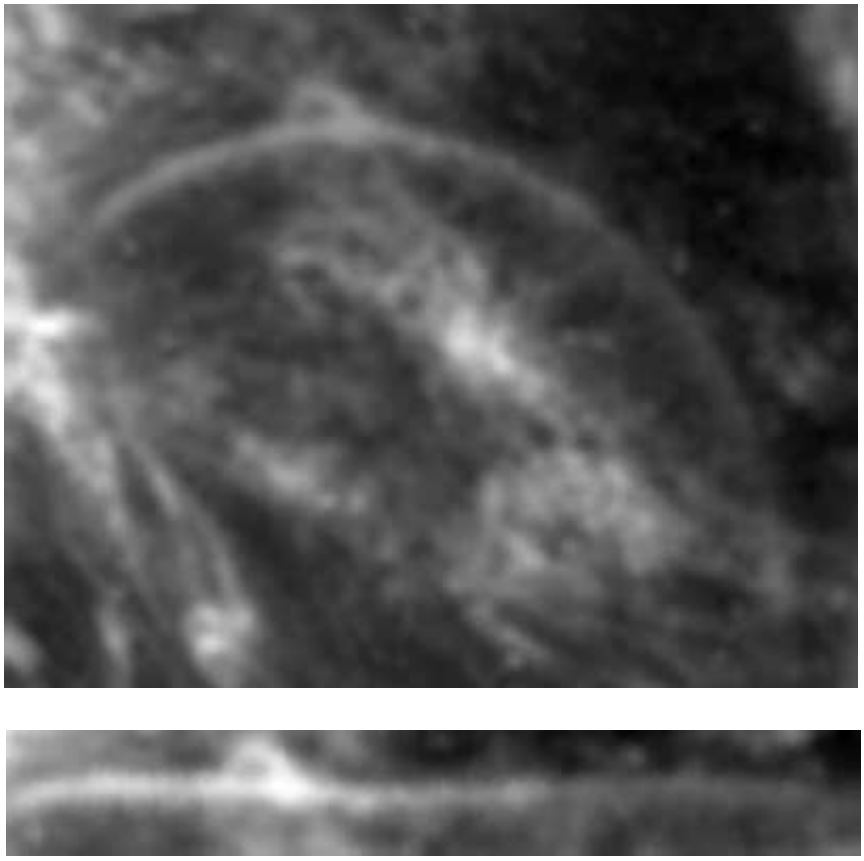

Fig. 1.— The loop shown is an example of the *TRACE* loops studied in LKD06. The lower panel shows the straightened version of the loop that is used for the width determination.

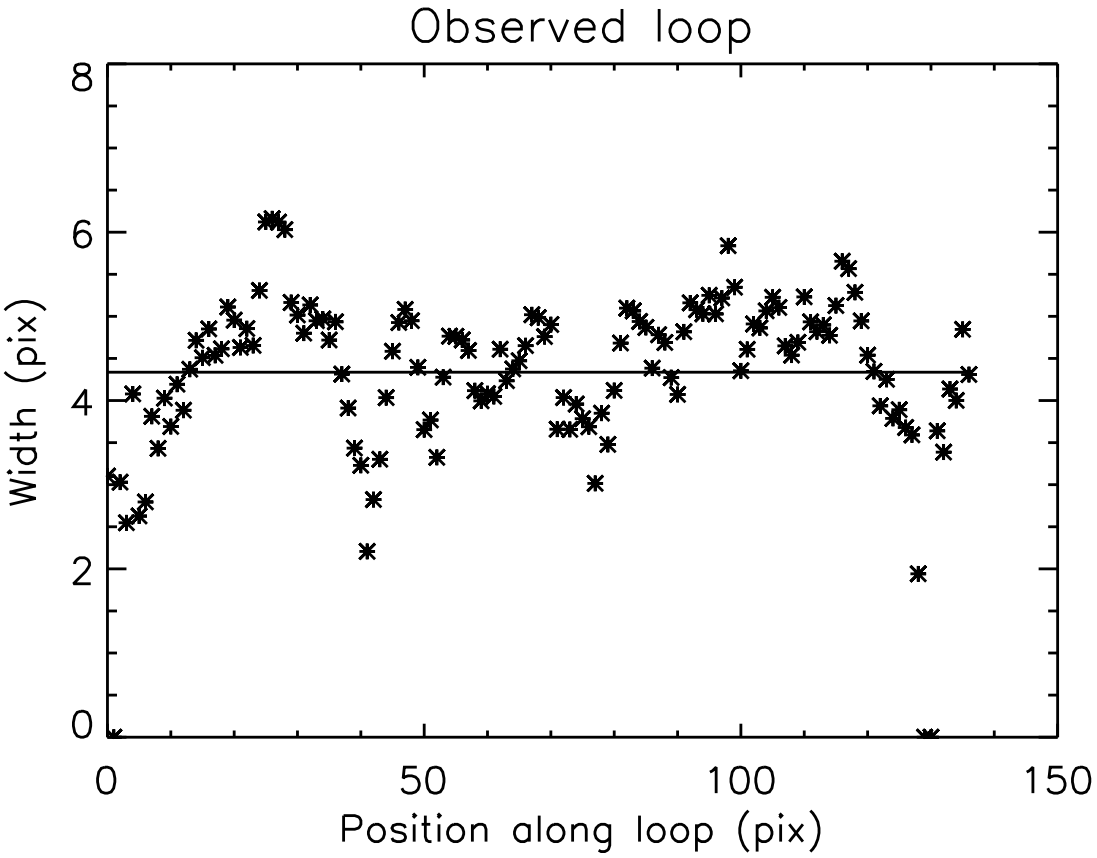

Fig. 2.— Measured width versus position along the loop of Figure 1. Background subtraction and PSF correction have been applied, as described in Section 2. The horizontal line shows the mean value.

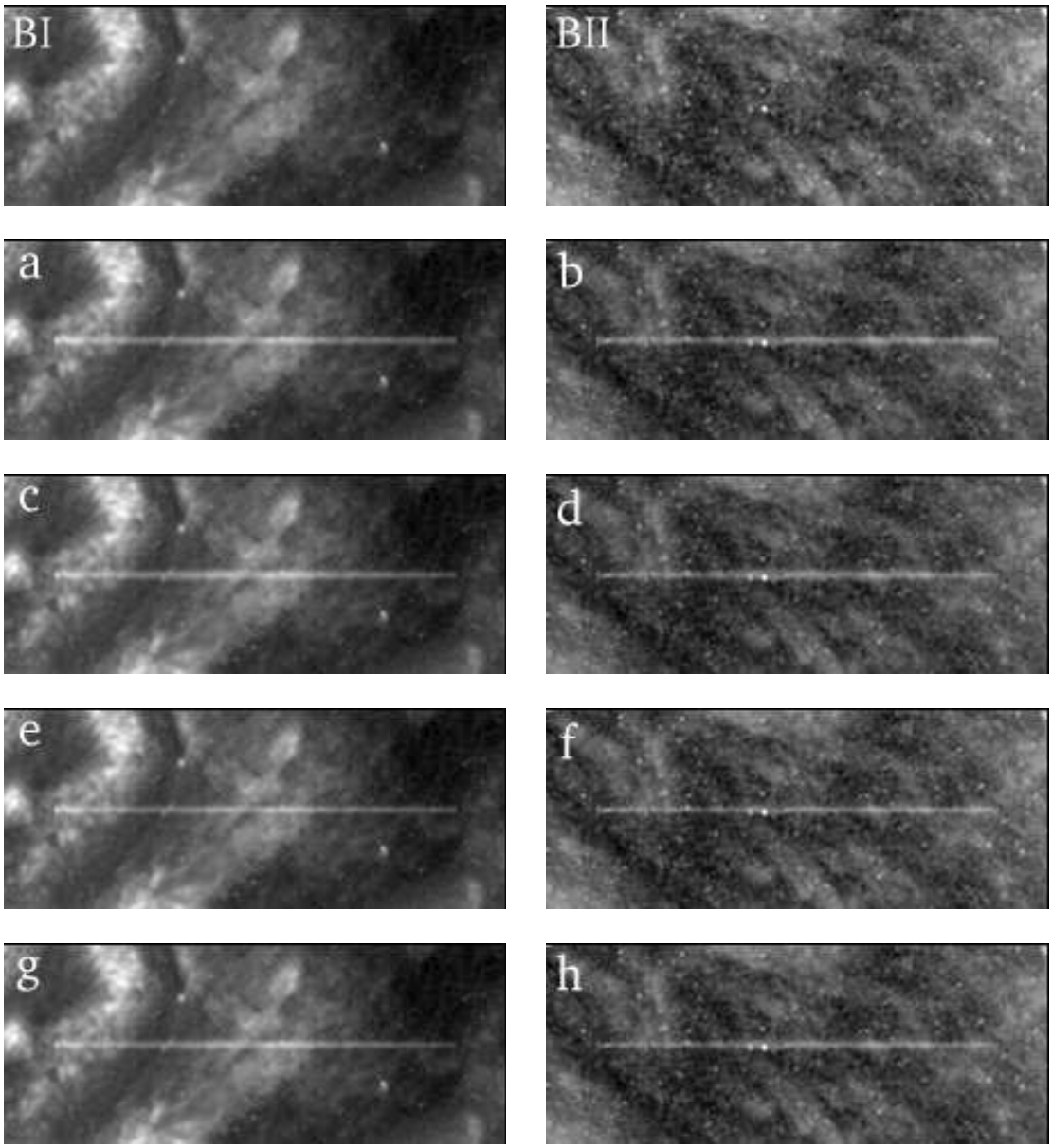

Fig. 3.— Synthetic data created by superposing loops with different specified properties on real *TRACE* backgrounds. The top panels show the background used in each column. The ends (footpoints) and middle of the loops have an imposed diameter (in pixels) of: (a,b) 4-4, (c,d) 2.5-5, (e,f) 3-3, (g,h) 2-4. This provides both constant and expanding (by a factor 2) synthetic loops close to the spatial resolution. For a detailed description of the panels see Section 3.

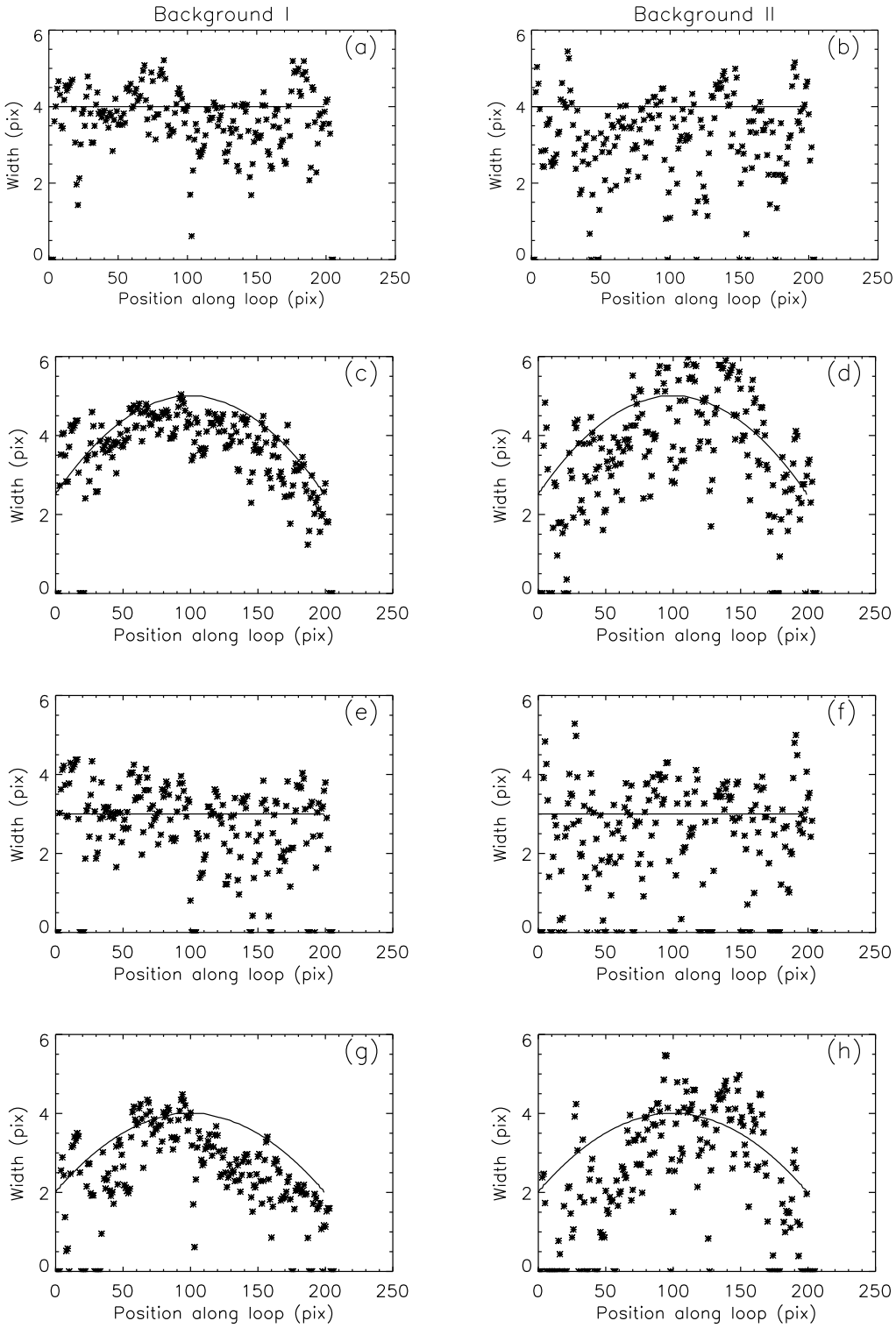

Fig. 4.— Measured width corrected for instrument resolution (asterisks) versus position along the synthetic loops shown in panels a) to h) of Figure 3. Continuous lines indicate the model width.

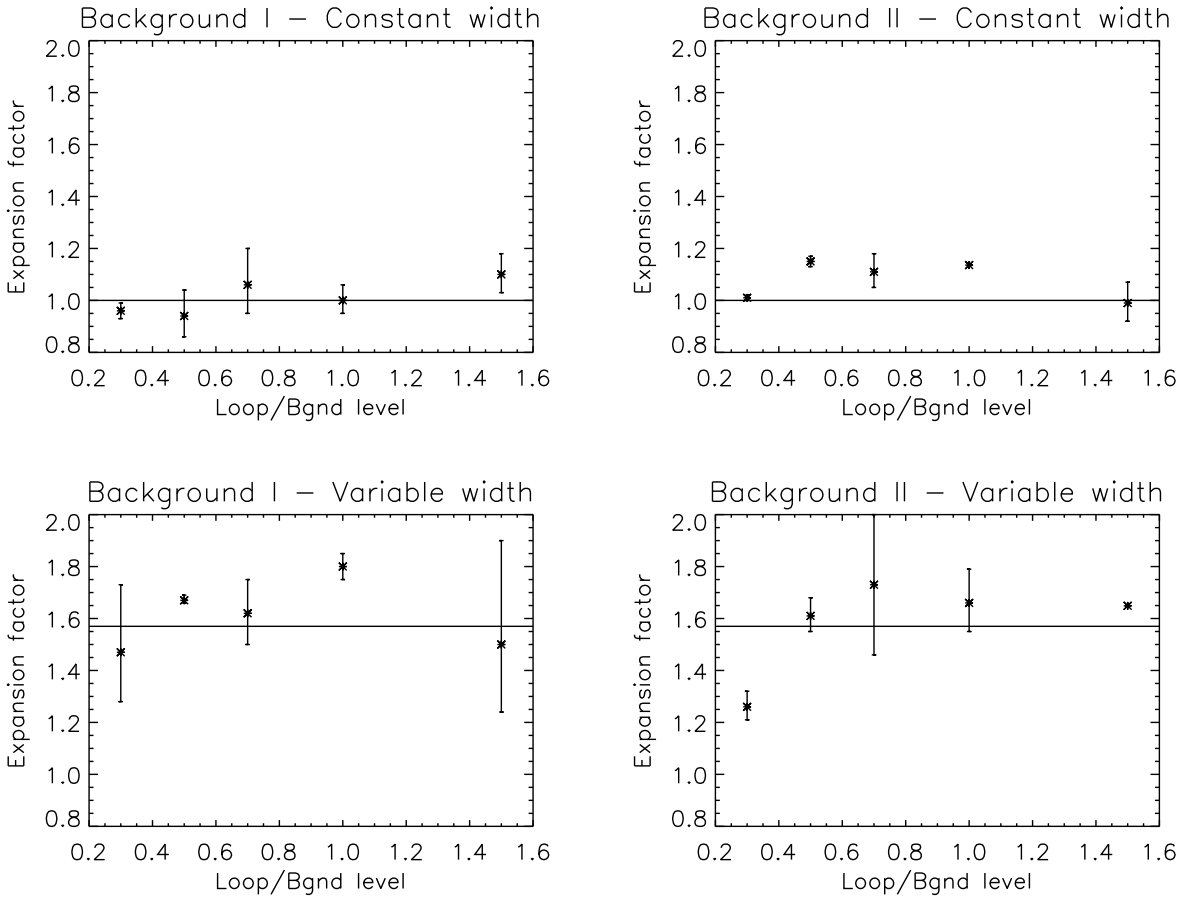

Fig. 5.— Expansion factor $\Gamma_{m/se}$ versus loop-to-background intensity ratio Φ, for expanding and non-expanding synthetic narrow loops on backgrounds I and II (similar to loops in panels e-h of Figure 4). The error bars are defined by the expansion factors $\Gamma_{m/s}$ and $\Gamma_{m/e}$ (see Section 4.1). The horizontal line indicates the expansion factor of the model.

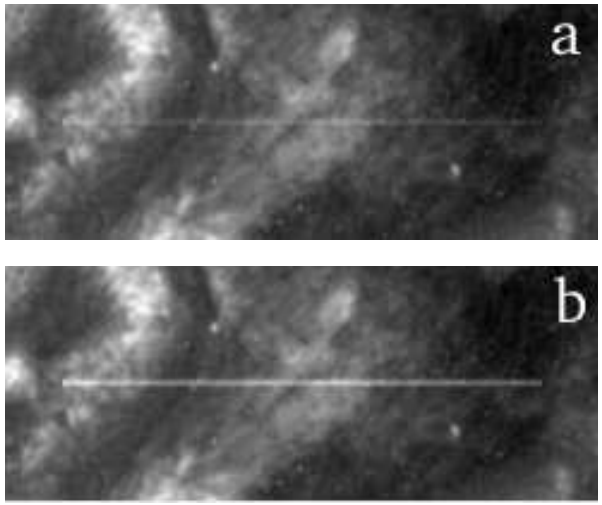

Fig. 6.— Two examples of unresolved synthetic loops constructed with a constant width of 0.5 pixels. The loops differ only in the loop-to-background intensity ratio Φ, which is set to 1 for case (a) and 3 for case (b) (see Section 4.1).

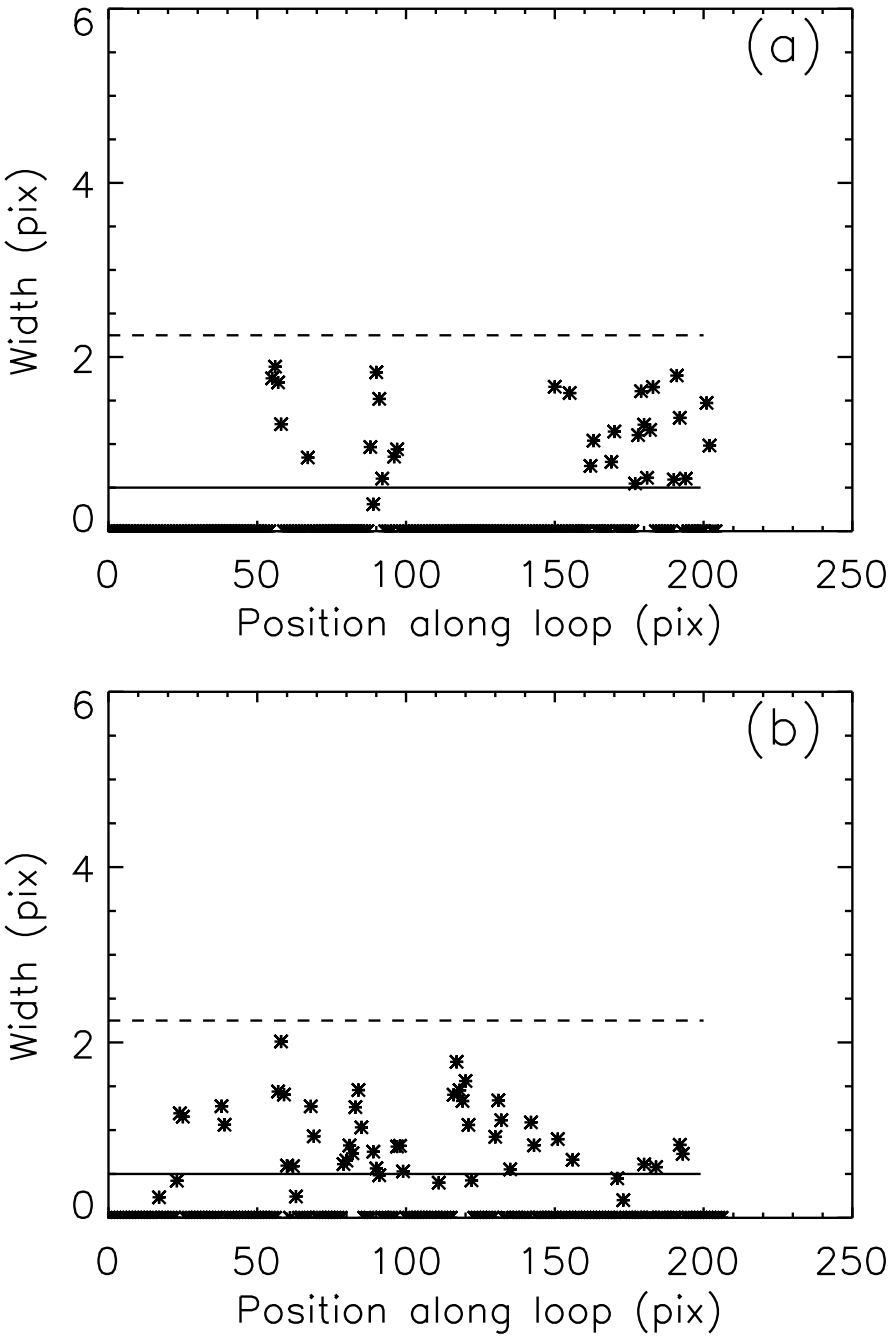

Fig. 7.— Width measurements for the two synthetic loops in Figure 6, corrected for the instrument resolution. The solid line indicates the actual model loop width, and the dashed line indicates the PSF full width at half maximum.

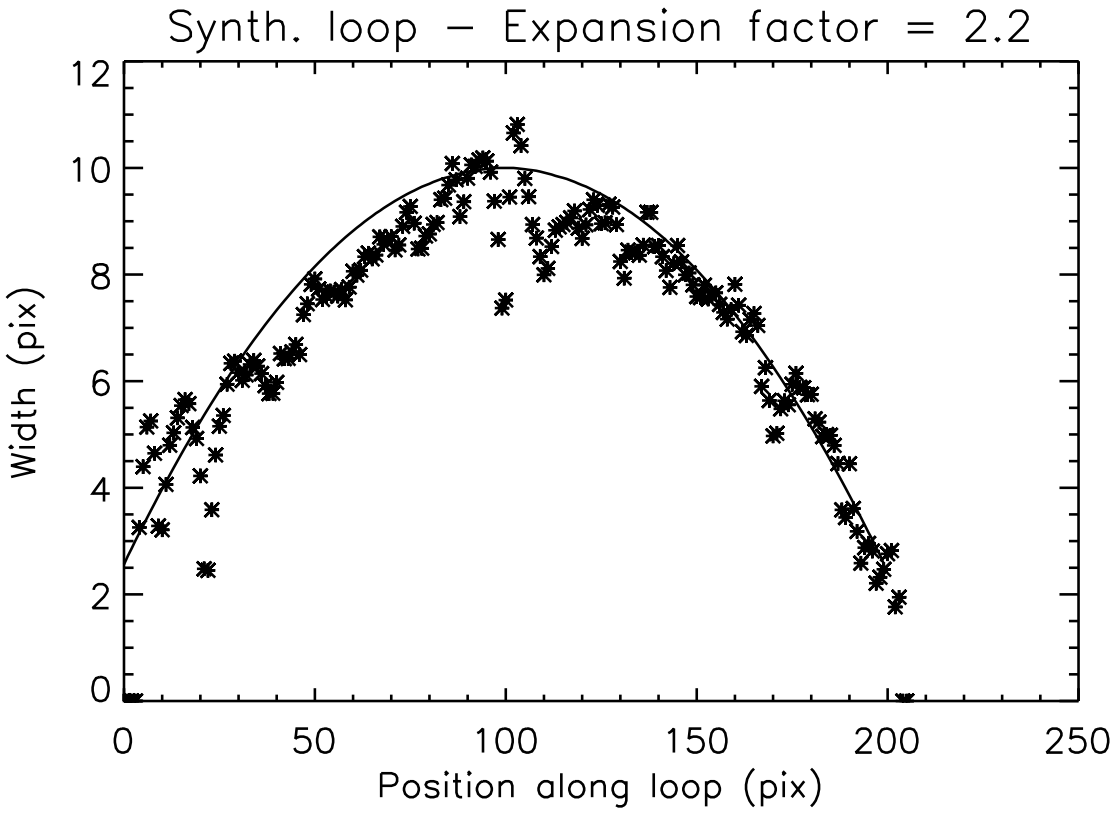

Fig. 8.— Width versus position along a synthetic loop with a model expansion factor of 2.2. The width has been corrected for instrument resolution.

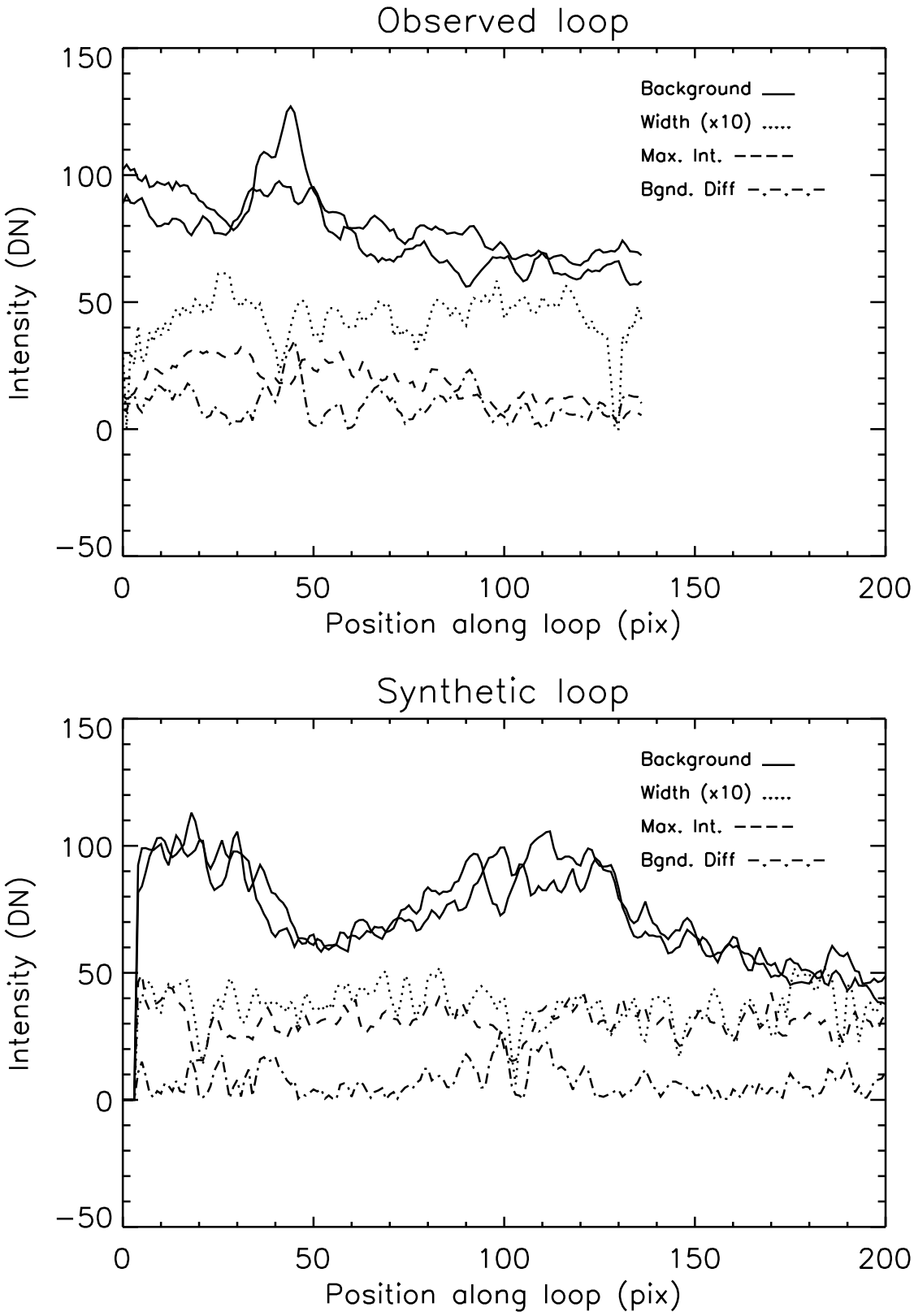

Fig. 9.— Different loop and background properties versus position along the loop. Top panel: example loop from Figure 1; botton panel: synthetic loop from Figure 3, panel a). For a detailed description see Section 4.2.

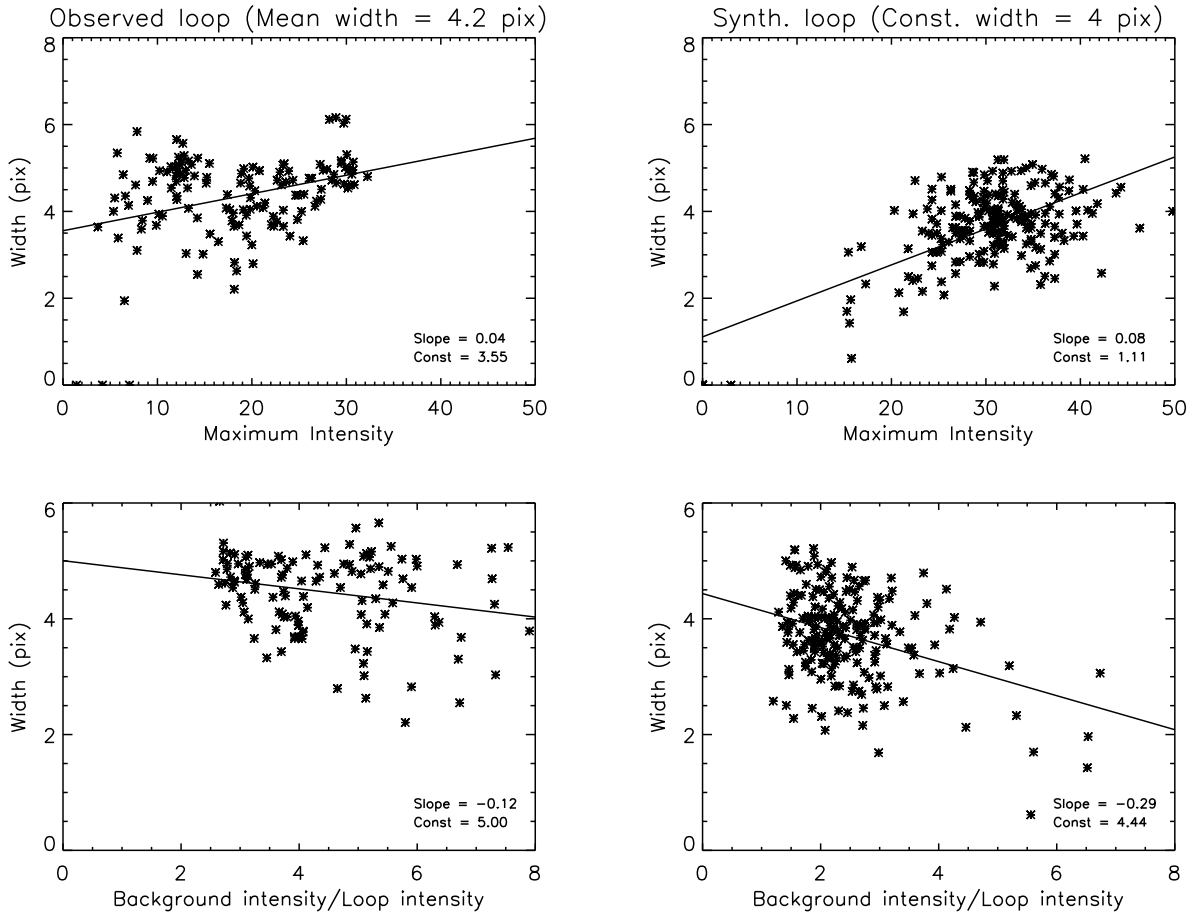

Fig. 10.— Scatter plots of measured quantities for the observed loop in Figure 1 (left column) and for the synthetic loop of Figures 3 and 4, panels (a) (right column). Top: width versus on-axis loop intensity. Bottom: width versus background intensity to loop intensity ratio (see Section 4.2). Continuous lines correspond to least-squares fits of the data. Slopes and intercepts are given in the respective panels.

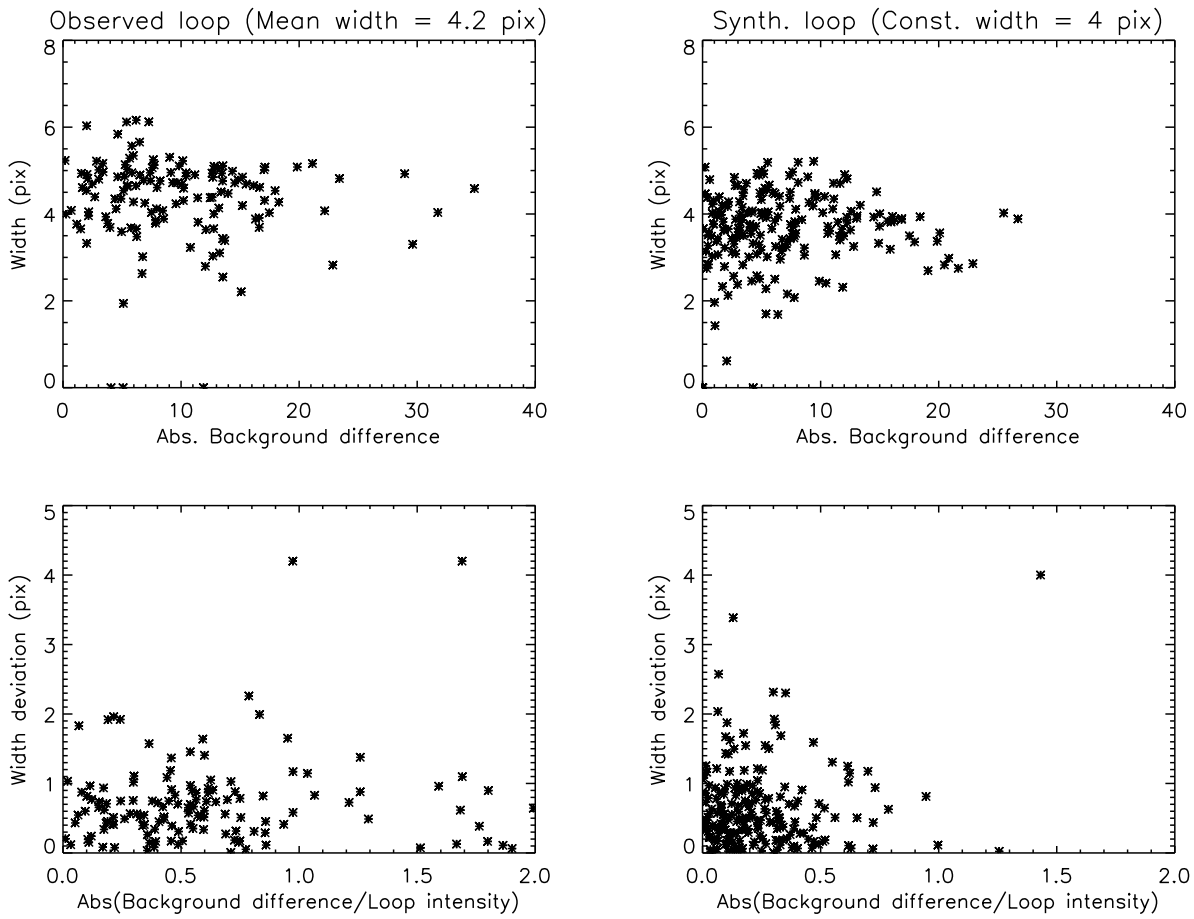

Fig. 11.— Scatter plots of measured quantities for the observed loop in Figure 1 (left column) and for the synthetic loop of Figures 3 and 4, panels (a) (right column). Top: width versus absolute value of the background intensity difference across the loop. Bottom left: width deviation from the mean versus the background intensity difference normalized by the loop intensity (see Section 4.2). Bottom right: same kind of plot, but the deviation is relative to the model width.